BULLETIN OF THE POLISH ACADEMY OF SCIENCES
TECHNICAL SCIENCES, Vol. 63, No. 4, 2015
*DOI: 10.1515/bpasts-2015-0101*

# Design of simultaneous input-shaping-based SIRMs fuzzy control for double-pendulum-type overhead cranes

D. QIAN[1]*, S. TONG[2], B. YANG[1], and S. LEE[3]

[1] School of Control and Computer Engineering, North China Electric Power University, Beijing 102206, P.R. China
[2] College of Automation, Beijing Union University, Beijing 100101, P.R. China
[3] Department of Electrical Engineering Yeungnam University, Gyeongsan, R. Korea

**Abstract.** Overhead cranes are extensively employed but their performance suffers from the natural sway of payloads. Sometime, the sway exhibits double-pendulum motions. To suppress the motions, this paper investigates the design of simultaneous input-shaping-based fuzzy control for double-pendulum-type overhead cranes. The fuzzy control method is based on the single input-rule modules (SIRMs). Provided the all the system variables are measurable, the SIRMs fuzzy controller is designed at first. To improve the performance of the fuzzy controller, the simultaneous input shaper is adopted to shape the control command generated by the fuzzy controller. Compared with other two control methods, i.e., the SIRMs fuzzy control and the convolved input-shaping-based SIRMs fuzzy control, simulation results illustrate the feasibility, validity and robustness of the presented control method for the anti-swing control problem of double-pendulum-type overhead cranes.

**Key words:** SIRMs fuzzy control, double-pendulum-type overhead cranes.

## 1. Introduction

Overhead cranes are widely used in many places, such as warehouses, disaster sites, nuclear plants, shipyards and construction sites, to transport objects because of their heavy payload capabilities [1, 2]. They are one of the most important elements in global industrialization and play an irreplaceable role in economic development. Structurally, a common characteristic among overhead cranes is that their payloads are supported via suspension cables, the cables are hanged on trolleys [3]. Although it provides the hoisting/lowering and moving functionalities of overhead cranes, such a characteristic also presents several challenges. The primary is the natural sway of payloads, which is inherently a pendulum-type motion [4]. The motion not only hazards safety but also degrades positioning accuracy. Experienced crane operators can eliminate the motion by moving the trolleys in small increments but this must result in an adverse effect on throughput and efficiency [5]. Thus, a large research effort is directed at automatic crane operation because high positioning accuracy, small swing angle, short transportation time, and high safety are required.

Recently, the study of overhead crane control approaches has received significant attention. Various methods concerning the control problem have been presented, i.e., fuzzy logic control [1–3], energy-based control [4], adaptive control [5], trajectory planning [6], input shaping [7], sliding mode control [8–10], to name but a few. See [11] for a review of these efforts in the crane control problem. In most of the reports about overhead crane control, including but not limited to [1–10], the mass-point assumption integrates all the suspending parts. The assumption leads to single-pendulum dynamics and most of the previous work on crane control has focused on how to resist the single-pendulum oscillations. However, double-pendulum dynamics actually exist because of certain types of payloads and cables [12]. The double-pendulum dynamics can degrade the effectiveness of those controllers for resisting the single-pendulum oscillations. Since they compound two kinds of pendulum motions with different natural frequencies, the double-pendulum oscillations are rather difficult to be eliminated. How to suppress the double-pendulum oscillations remains challenging [13].

Some researchers have presented several methods to attack the issue, i.e., decoupling control [14], passivity-based control [15], wave-based control [16], hierarchical sliding mode control [17, 18], input shaping control [12, 13, 19–23], neural-network-based intelligent control [24], e ct. The methods can roughly be divided into two categories according to the type of control structure, i.e., feedback control [14–18, 24] or feedforward control [12, 13, 19–23]. Any method has both merits and drawbacks. As Singhose and his colleagues [13] pointed out, feedback control is challenging due to the difficulty of measuring the payload motion but feedforward control has to tolerate a level of residual vibration because of modeling errors and unmodelled actuator dynamics.

The motivation of the paper does not advocate or compare which control structure is superior, but rather investigates a possible design for the anti-wing control problem of double-pendulum-type overhead cranes. Consequently, the structure of feedback control is adopted under the assumption that all the system variables are measurable. With the development of sensor and measuring technology, it is probable and fea-

*e-mail: dianwei.qian@ncepu.edu.cn

sible to utilize the feedback structure for double-pendulum-type overhead crane control although currently measuring the double-pendulum motions is difficult.

As a model-free approach, fuzzy control [25] has been proven to be effective for solving unmodelled dynamics. However, the method suffers from the problem of exponential rule explosion [26]. To avoid the problem, the single-input-rule modules (SIRMs) method was addressed by Yi et al. [27]. So far, the SIRMs method has been successfully implemented on cart-pole system [27], medical diagnosis system [28], fuel cell system [29] and stress prediction system [30]. Although the SIRMs method [2] in 2003 was carried out by a single-pendulum-type overhead crane, how to establish the SIRMs of double-pendulum-type overhead cranes still remains untouched and problematic due to the challenge and complexity of double-pendulum dynamics.

This paper touches the topic. To develop the SIRMs fuzzy control for double-pendulum-type overhead cranes, six dynamically-weighted SIRMs are introduced to archive the anti-swing control in the form of feedback control. To optimize the control command generated by the fuzzy controller, a simultaneous input shaper is employed as feedforward control. According to such a design scheme, the two control methods fuse together by means of the types of their control structures. Compared with the sole SIRMs fuzzy control and the convolved input-shaping-based SIRMs fuzzy control, the feasibility, validity, and robustness of the compound control method are illustrated by numerical simulation results.

The remainder of this paper is organized as follows. Section 2 describes dynamics of double-pendulum-type overhead crane systems. The control design is presented in Sec. 3. Section 4 demonstrates the numerical simulation results. Conclusion is drawn in Sec. 5 at last.

## 2. Dynamics of double-pendulum-type overhead crane systems

Figure 1 illustrates the schematic representation of a double-pendulum-type overhead crane. Such a system is underactuated [31] and consists of three subsystems: trolley, hook and payload. Each subsystem can be described by one generalized coordinate variable such that the following three generalized coordinate variables exist to describe the motion equations of the crane. $x$ (m) depicts the trolley position with respect to the origin. $\theta_1$ (rad) and $\theta_2$ (rad) are the swing angles with respect to the vertical line and they describes the double pendulum motions of the other two subsystems.

Further, the rest of symbols in Fig. 1 are explained as follows. The crane is moved by a driven force $F$ (N), applied to the trolley of mass $m$ (kg). A cable of length $l_1$ (m) hangs below the trolley and supports a hook, of mass $m_1$ (kg). The rigging below the hook is modeled as a second cable of length $l_2$ (m). The payload is of mass, $m_2$ (kg).

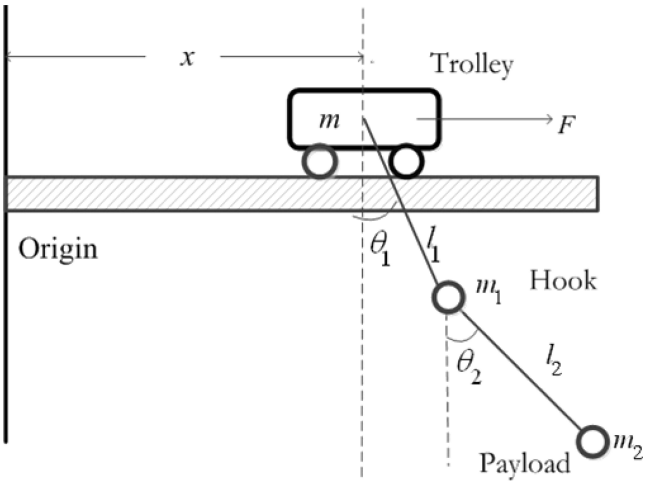


Fig. 1. Schematic of double-pendulum-type overhead crane system

Provided that no friction, massless and rigid cables, mass-point hook and mass-point payload, the equations of motion with zero initial conditions [15] can be obtained by Lagrange's method.

$$\mathbf{M}(\mathbf{q})\,\ddot{\mathbf{q}} + \mathbf{C}(\mathbf{q},\dot{\mathbf{q}})\,\dot{\mathbf{q}} + \mathbf{G}(\mathbf{q}) = \boldsymbol{\tau}. \tag{1}$$

Here $\mathbf{q} = \begin{bmatrix} x & \theta_1 & \theta_2 \end{bmatrix}^T$ is a vector of the three generalized coordinates, $\boldsymbol{\tau} = \begin{bmatrix} F & 0 & 0 \end{bmatrix}^T$ is a vector of the generalized force, $g$ is the gravitational acceleration, $\mathbf{M}(\mathbf{q})$ is a $3 \times 3$ inertia matrix, $\mathbf{C}(\mathbf{q},\dot{\mathbf{q}})\,\dot{\mathbf{q}}$ is a vector of Coriolis and centripetal torques, $\mathbf{G}(\mathbf{q})$ is a vector of the gravitational term. $\mathbf{M}(\mathbf{q})$, $\mathbf{C}(\mathbf{q},\dot{\mathbf{q}})$ and $\mathbf{G}(\mathbf{q})$ are determined by

$$\mathbf{M}(\mathbf{q}) = \begin{bmatrix} m+m_1+m_2 & (m_1+m_2)l_1\cos\theta_1 & m_2 l_2\cos\theta_2 \\ (m_1+m_2)l_1\cos\theta_1 & (m_1+m_2)l_1^2 & m_2 l_1 l_2\cos(\theta_1-\theta_2) \\ m_2 l_2\cos\theta_2 & m_2 l_1 l_2\cos(\theta_1-\theta_2) & m_2 l_2^2 \end{bmatrix},$$

$$\mathbf{C}(\mathbf{q},\dot{q}) = \begin{bmatrix} 0 & -(m_1+m_2)l_1\dot{\theta}_1\sin\theta_1 & -m_2 l_2\dot{\theta}_2\sin\theta_2 \\ 0 & 0 & m_2 l_1 l_2\dot{\theta}_1\sin(\theta_1-\theta_2) \\ 0 & -m_2 l_1 l_2\dot{\theta}_1\sin(\theta_1-\theta_2) & 0 \end{bmatrix},$$

$$\mathbf{G}(\mathbf{q}) = \begin{bmatrix} 0 & (m_1+m_2)gl_1\sin\theta_1 & m_2 g l_2\sin\theta_2 \end{bmatrix}^T.$$

## 3. Control design

Fuzzy control is a model-free method. This appears to be beneficial both for control design and analysis. But the method is criticized for its exponential rule explosion [1]. The SIRMs fuzzy method presented by Yi et al. [2] can dramatically reduce the numbers of rules and parameters. This section develops such a fuzzy controller for the crane in Fig. 1. The controller is composed of six dynamically-weighted SIRMs. Note the crane model (1) is only prepared for simulation studies. The following control design assumes that the model is completely unknown.

**3.1. Dynamically-weighted SIRMs method** To develop a SIRMs fuzzy controller, a briefly introduction of the dynamically- weighted SIRMs method is presented at first. To formulate the method, the $i$-th single-input-rule module (SIRM) is defined by

$$\mathrm{SIRM}-i: \left\{ \mathrm{R}_i^j: \quad \text{if } x_i = A_i^j \text{ then } \quad f_i = C_i^j \right\}_{j=1}^{m_i}. \tag{2}$$

Here $\mathrm{SIRM}-i$ is a SIRM to depict the $i$-th input item of the designed fuzzy inference system; $\mathrm{R}_i^j$ is the $j$-th rule of $\mathrm{SIRM}-i$; $x_i$ and $f_i$ are the antecedent and consequent variables of the $i$th input item, respectively, where $f_i$ is also an intermediate variable corresponding to the output item $f$; $A_i^j$ and $C_i^j$ are the membership functions of $x_i$ and $f_i$, respectively. In (2), $i = 1, 2, 3, \cdots, n$ denotes the index number of SIRMs and $j = 1, 2, 3, \cdots, m_i$ denotes the rule number of $\mathrm{SIRM}-i$. In $\mathrm{SIRM}-i$, the inference result $f_i^0$ of the consequent variable $f_i$ can be formulated by

$$f_i^0 = \frac{\sum_{j=1}^{m_i} A_i^j(x_i) C_i^j}{\sum_{j=1}^{m_i} A_i^j(x_i)}. \tag{3}$$

Each input item plays a unique role in system performance. To describe the important rank of the $i$-th input item, its dynamic weight $w_i^D$ is defined in (4). Note that $w_i^D$ is independent on $x_i$

$$w_i^D = w_i + B_i \Delta w_i^0. \tag{4}$$

In (4), $w_i$ denotes a base value and it guarantees the $i$-th input item plays the basic role. $\Delta w_i^0$ is a dynamic variable. $\Delta w_i^0$ varies from 0 to 1 and it can be automatically adjusted by means of predefined fuzzy rules. Finally, the output item $f$ of the whole $n$ SIRMs has a form of

$$f = \sum_{i=1}^{n} w_i^D f_i^0. \tag{5}$$

Here $f_i^0$ is the fuzzy inference result of $\mathrm{SIRM}-i$.

**3.2. Design of SIRMs fuzzy controller.** Concerning the crane in Fig. 1, its control task is to transport the payload to a required position as fast and accurately as possible. Meanwhile, the designed controller has to suppress the double-pendulum-type oscillations induced by the trolley motions. The trolley motions are driven by the force $F$. To achieve the compound control task, $F$ is picked up as the control input applied to the trolley. Without loss of generality, define $x \in \left[ \begin{array}{cc} -1\ \mathrm{m} & 1\ \mathrm{m} \end{array} \right]$, $\theta_1 \in \left[ \begin{array}{cc} -0.5\ \mathrm{rad} & 0.5\ \mathrm{rad} \end{array} \right]$ and $\theta_2 \in \left[ \begin{array}{cc} -0.5\ \mathrm{rad} & 0.5\ \mathrm{rad} \end{array} \right]$. If any of the three variables gets out of its predefined intervals, then the control process is regarded as a failure.

As far as the crane is concerned, its control input $F$ covers three parts, i.e., trolley position control, hook angle control and payload angle control. In order to simultaneously cover the three types of controls, $x$, $\dot{x}$, $\theta_1$, $\dot{\theta}_1$, $\theta_2$ and $\dot{\theta}_2$ in (1) are treated as controller inputs. Accordingly, the control input $F$ is undoubtedly the sole controller output. The scaling factors of the six controller inputs in order are fixed to 1.0 m, 1.0 m/s, 0.5 rad, 1.5 rad/s, 0.5 rad and 1.5 rad/s although the exact values of the maximum velocity and angular velocity are unknown. The scaling factor of $F$ is set up to $1.5(m+m_1+m_2)$.

Assume $x$, $\dot{x}$, $\theta_1$, $\dot{\theta}_1$, $\theta_2$ and $\dot{\theta}_2$ are measurable. Having been normalized by their own private scaling factors, the six variables are selected in order as the input items $x_i (i = 1, 2, \cdots, 6)$, and the driven force $F$ is set as the output item $f$. The six variables and the driven force determine the controller inputs and the controller output, respectively. In such a manner, the designed SIRMs fuzzy inference system takes normalized 6 input items and 1 output item. Since one dynamically-weighted SIRM is assigned to each input item, six SIRMs have to be designed.

Although the controller inputs, the control input and the input items have different meanings they have particular relevance to the crane control problem. The control input applied to the trolley is calculated by means of the controller inputs. Having been normalized, the controller inputs become the input items that are the antecedent variables of the designed SIRMs-based fuzzy inference system.

**Setting the SIRMs.**

Six SIRMs exist in the designed fuzzy inference system. Each module employs fuzzy rules to achieve its own inference processing. The fuzzy rules should be drawn by analyzing the relation between the input item of each module and the control performance. The analysis originates from experience and intuition because of the assumption that the crane dynamics are completely unknown.

Yi et al. [2] proposed how to set SIRMs for a single-pendulum-type overhead crane. Although some results in [2] are referential, how to suppress the double-pendulum-type motions still remains untouched and problematic. Partly, the complexity of the double-pendulum dynamics is an obstacle.

**Analysis of the trolley position control.** This control includes two modules, i.e., SIRM-1 and SIRM-2. According to the Newton's second law, $x_1$ and $f_1$ in SIRM-1 should be opposite in direction but they should be of same tendency in magnitude to achieve the trolley position control. Concerning SIRM-2, a similar conclusion can be reached. The linguistic description is available in [2].

**Analysis of the hook-angle and payload-angle controls**. Because the sole control input achieves all the three con-

trols, the two angle controls are not only coupled to each other, but also they are coupled to the trolley position control. To establish the fuzzy rules for their SIRMs, the two angle controls are mandatorily decoupled and the double-pendulum motions are treated as two independent single-pendulum motions. Yi et al. [2] realized the angle control by establishing SIRMs for a single-pendulum overhead crane. Briefly, $x_i$ and $f_i$ $(i = 3, 4, 5, 6)$ in SIRM-$i$ should be same in direction and should be of same tendency in magnitude. The linguistic description is available in [2].

According to the above analysis, the fuzzy rules of $x_1$ and $x_2$ are set up in Table 1 and the fuzzy rules of $x_3$, $x_4$, $x_5$ and $x_6$ are set up in Table 2. Here, $f_i$ $(i = 1, 2, \cdots, 6)$ is the fuzzy inference result of each SIRM and they are intermediate variables corresponding to the output item $f$; NB, ZO and PB are linguistic labels and they denote negative big, zero and positive big, respectively; the membership functions of the labels for all the input items are defined in Fig. 2.

Table 1
SIRMs for the trolley

| Antecedent variable $x_i$ $(i = 1, 2)$ | Consequent variable $f_i$ $(i = 1, 2)$ |
|---|---|
| NB | 1.0 |
| ZO | 0.0 |
| PB | $-1.0$ |

Table 2
SIRMs for the hook and payload

| Antecedent variable $x_i$ $(i = 3, 4, 5, 6)$ | Consequent variable $f_i$ $(i = 3, 4, 5, 6)$ |
|---|---|
| NB | $-1.0$ |
| ZO | 0.0 |
| PB | 1.0 |

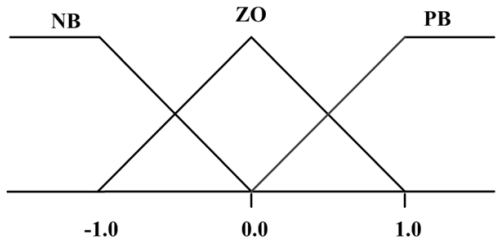

Fig. 2. Membership functions of each SIRM

**Contradiction.** Suppose that the crane in Fig. 1 is static, that the trolley is located at the origin and that the hook and payload are in their downward positions. If a positive driven force is added to the trolley, then the trolley will moves toward the right direction. Simultaneously, the hook will rotate clockwise and the payload will rotate counterclockwise. Apparently, the tendency of the hook-angle and payload-angle controls should be opposite. However, the two angle controls are mandatorily endowed with the same fuzzy rules. The contradiction between the fuzzy rules and the real tendency is regulated by the following dynamic weights.

**Setting the dynamic weights.**

As mentioned, each input item plays a unique role in the crane control system. The role is exhibited by degree of importance. The degree of importance of an input item is described by its dynamic weight. Generally speaking, the bigger the dynamic weight is, the higher priority the corresponding input item has.

A dynamic weight defined in (4) has three parameters, i.e. basic value $w_i$, breadth $B_i$ and inference result $\Delta w_i^0$, where $\Delta w_i^0$ is determined by fuzzy rules. To establish the fuzzy rules, it is necessary to analyze the three controls according to experience and intuition. To solve the aforementioned contradiction, the four dynamic weights about the hook-angle and payload-angle controls are considered at first.

Intuitively, the crane control system probably fails if the hook angle or angular velocity is large. However, the control system possibly works if the payload angle or angular velocity is large. In light of this intuition, the hook angle control should have a higher priority. On the other hand, when the hook angle or angular velocity is small, the priority of the payload angle control should be increased because the double-pendulum-type crane tends to be stable under this circumstance. As a result, $|x_3|$ is selected as the antecedent variable. The four dynamic weights about the two angle controls are determined by Tables 3 and 4, respectively.

Although it facilitates the SIRMs design, the fuzzy rules derived from mandatory decoupling conflict with the double-pendulum-type motions. The contradiction is tuned by designing the dynamic weights in Tables 3 and 4. From Table 4, the payload control is injected into the control input by increasing the dynamic variables $\Delta w_5^0$ and $\Delta w_6^0$ when the hook angle is small; the payload control is not taken into consideration under other circumstances. Such fuzzy rules in Table 4 decouple two independent single-pendulum-type motions from the double-pendulum-type motions.

Table 3
Dynamic weights for the hook

| Antecedent variable $\lvert x_3\rvert$ | Consequent variables $\Delta w_3^0$ and $\Delta w_4^0$ |
|---|---|
| S | 0.0 |
| M | 0.5 |
| B | 1.0 |

Table 4
Dynamic weights for the payload

| Antecedent variable $\lvert x_3\rvert$ | Consequent variables $\Delta w_5^0$ and $\Delta w_6^0$ |
|---|---|
| S | 1.0 |
| M | 0.0 |
| B | 0.0 |

To establish the left two dynamic weights of the trolley position control, the physical property of the double-pendulum-type overheard crane is considered. Concerning the crane, the sole control input, directly applied to the trolley, indirectly affects the other two controls by the couplings among the three

controls. To suppress the double-pendulum motions, the importance of the trolley position control cannot be increased when either $|x_{3|}$ or $|x_5|$ is big. On the other hand, the importance can only be strengthened when both $|x_3|$ and $|x_5|$ are small. To exhibit the couplings, the absolute values of $|x_3|$ and $|x_5|$ are selected as the antecedent variables. The two dynamic weights about the trolley position control are determined by Table 5. From Table 5, it is found that the trolley control is cut off if either of the angles is big and that the trolley control is triggered by increasing dynamic variables $\Delta w_1^0$ and $\Delta w_2^0$ if both the angles are small.

S, M and B in Tables 3–5 are linguistic labels and they denote small, middle, and big, respectively. The membership functions of the linguistic labels for all the input items are defined in Fig. 3.

Table 5
Fuzzy rules of two dynamic weights for the trolley control

| Consequent variables $\Delta w_1^0$ and $\Delta w_2^0$ | | Antecedent variable $\|x_3\|$ | | |
|---|---|---|---|---|
| | | S | M | B |
| Antecedent variable $\|x_5\|$ | S | 1.0 | 0.5 | 0.0 |
| | M | 0.5 | 0.0 | 0.0 |
| | B | 0.0 | 0.0 | 0.0 |

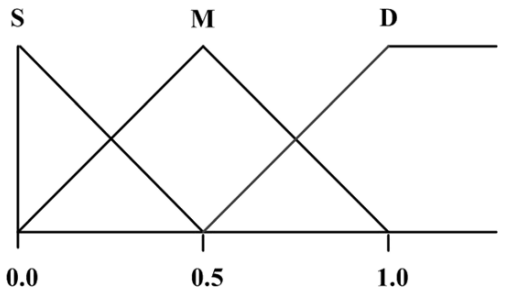

Fig. 3. Membership functions of each dynamic variable

**3.3. Design of simultaneous input shaper.** Input shaping is a control technique for reducing vibrations. The method works by creating a command signal, where vibration caused by the first part of the command signal is canceled by vibration caused by the second part of the command signal. The input shaping method has proven effective for controlling oscillations of several types of cranes [7, 12, 13, 20–22].

The double-pendulum-type crane in Fig. 1 has two natural frequencies. The two frequencies of the double-pendulum dynamics modeled in (1) can be derived from linearizing (1) around $\theta_1 = 0$ and $\theta_2 = 0$. They are formulated by

$$\begin{aligned} \varpi_1 &= \sqrt{\frac{g}{2}}\sqrt{(1+R)\left(\frac{1}{l_1}+\frac{1}{l_2}\right)+\beta} \\ \text{and } \varpi_2 &= \sqrt{\frac{g}{2}}\sqrt{(1+R)\left(\frac{1}{l_1}+\frac{1}{l_2}\right)-\beta}, \end{aligned} \tag{6}$$

where $g$ is the gravitational acceleration, $R$ is the payload-to-hook mass ratio and

$$\beta = \sqrt{(1+R)^2\left(\frac{1}{l_1}+\frac{1}{l_2}\right)^2 - 4\left(\frac{1+R}{l_1 l_2}\right)}.$$

W. Singhose et al. [13] discussed the function relation between the two frequencies and the payload-to-hook mass ratio, the lengths of the two cables in detail.

To resist the two-frequency oscillations in (6), one can consider the design of convolved or simultaneous input shapers where convolved shapers are easy to design but simultaneous shapers are faster [13]. Proven in [13], the maximum amplitude of the residual vibration originates from a series of impulses and the maximum amplitude can be calculated by adding the maximum amplitudes from each frequency, which has the form of

$$V_{amp} = |C_1| + |C_2| \tag{7}$$

Here

$$C_1 = \frac{\omega_1 l_1 \left[1+\omega_2\alpha\left(l_1+l_2\right)\right]}{k} \cdot \sqrt{\left(\sum_{j=1}^{n} A_j \cos\omega_1 t_j\right)^2 + \left(\sum_{j=1}^{n} A_j \sin\omega_1 t_j\right)^2},$$

$$C_1 = -\frac{\omega_2 l_1 \left[1+\omega_1\alpha\left(l_1+l_2\right)\right]}{k} \cdot \sqrt{\left(\sum_{j=1}^{n} A_j \cos\omega_2 t_j\right)^2 + \left(\sum_{j=1}^{n} A_j \sin\omega_2 t_j\right)^2},$$

$\alpha = -\dfrac{g\left(1+R\right)}{\omega_1^2\omega_2^2 l_1 l_2}$, $k = \beta l_1 g$ and $A_j$ is an impulse of magnitude.

To achieve the crane control task mentioned in Subsec. 3.2, the simultaneous input shaping method is employed to shape the command generated by the SIRMs fuzzy control. The basic idea of the simultaneous input shaper is to make the shaper duration $t_n$ in (7) as short as possible. Briefly, the shaper design is to minimize the time of the input shaper impulse subject to some constraints. As a result, the objective function is formulated by

$$\min t_n, \tag{8}$$

(8) is subject to two types of constraints. They are residual vibration constraint and amplitude constraint, described by

$$V_{amp} \le V_{tol}, \tag{9}$$

$$\sum_{i=1}^{n} A_i = 1 \quad \text{and} \quad A_i > 0. \tag{10}$$

Here $V_{tol}$ depicts the residual oscillations expressed with a unit of length.

**3.4. Analysis of control system structure.** The structure of the simultaneous-input-shaping-based SIRMs fuzzy control system is presented in Fig. 4. From Fig. 4, $x$, $\dot{x}$, $\theta_1$, $\dot{\theta}_1$, $\theta_2$ and $\dot{\theta}_2$ are located at the feedback channel. Having been subtracted by the corresponding reference inputs, the errors of the six variables become the inputs of the normalizer (NL) block. Having been normalized, the fuzzy input items, $x_i (i = 1, 2, \cdots, 6)$, are obtained.

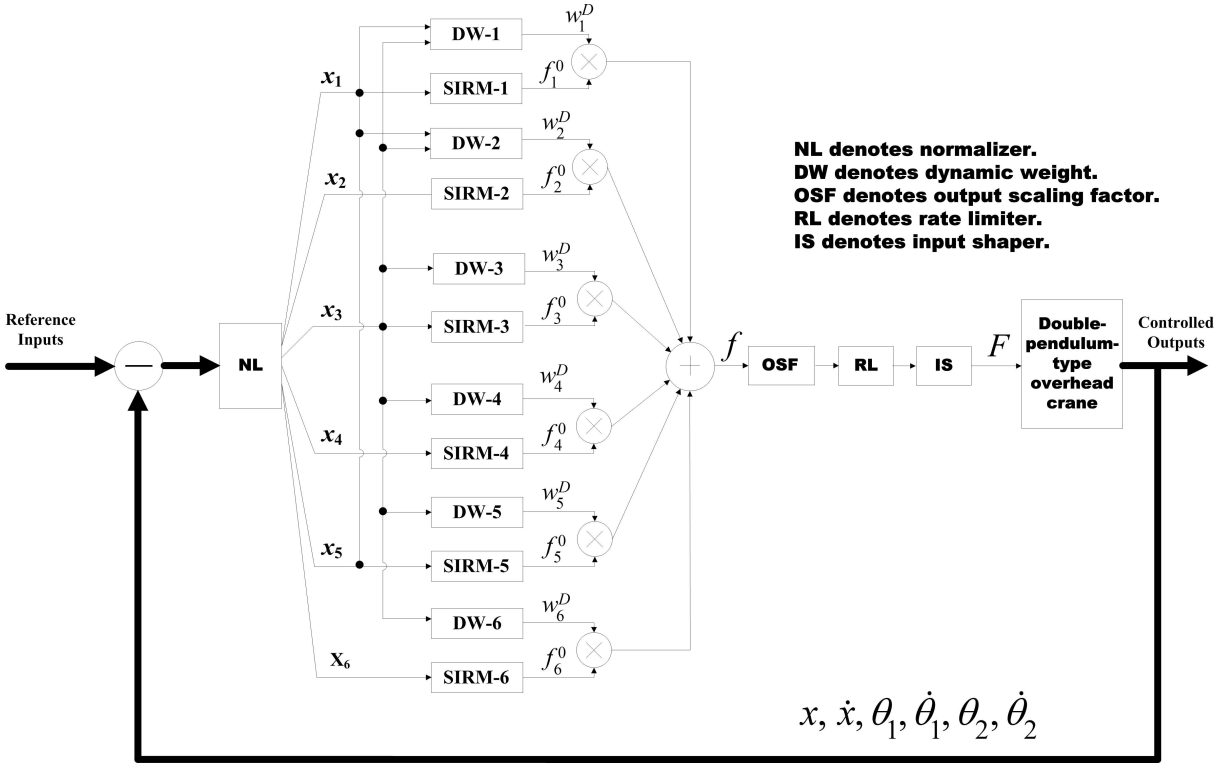


Fig. 4. Block diagram of the simultaneous input-shaping-based SIRMs fuzzy control system

The input item $x_i$ feeds the SIRM-$i$ block and the output of the SIRM-$i$, $f_i$, is derived from the designed fuzzy rules. Both $x_3$ and $x_5$ feed the dynamic-weight (DW) blocks of the trolley position control as the antecedent variables. The DW blocks of the hook angle control employ the input item $x_3$ as the antecedent variable, so do the DW blocks of the payload angle control.

Summing each output of the SIRM-$i$ block, $f_i$ times the output of its own DW block, $w_i^D$, we can obtain the output item $f$ of this SIRMs-based fuzzy inference system. Inputting $f$ to the output scaling factor (OSF) block and passing the OSF output through the rate limiter (RL) block yields the control command generated by the SIRMs fuzzy control method. The control command is shaped by the simultaneous input shaper (IS) block. Finally, the control input, driven force $F$, can be obtained. Here the function of the RL block is served to improve the system performance by resisting the control input swinging rapidly back and forth.

## 4. Simulation results

In this section, the simultaneous input-shaping-based SIRMs fuzzy controller will be applied to the point-to-point transport control of the double-pendulum-type overhead crane system in Fig. 1. Pointed out in [13], shaping is necessary for double-pendulum-type overhead crane systems with low payload-to-hook mass ratios. In Fig. 1, the physical parameters are determined by $m = 0.5$ kg, $m_1 = 0.25$ kg, $m_2 = 0.5$ kg, $l_1 = 0.5$ m and $l_2 = 0.5$ m, which are treated as nominal ones. Note that the payload-to-hook mass ratio is 2 and the two cables length ratio $l_2/l_1$ is 1. Both the ratios are selected from a benchmark, reported by Singhose et al. [13].

The scaling factors of the input items are defined in Sec. 3, so the scaling factor of the output item is. The base value and the breadth of each input item are shown in Table 6. The rate of the rate limiter in Fig. 4 is set as 6. The simultaneous input shaper is obtained by minimizing (8) subject to (9) and (10), where $V_{tol}$ in (9) is set as 5%, meaning the shaper is designed to accommodate 5% variations in both the low and high frequencies. Using the MATLAB optimization toolbox, the designed input shaper contains five impulses as follows.

$$\begin{bmatrix} A_i \\ t_i \end{bmatrix} = \begin{bmatrix} 0.2152 & 0.2848 & 0.0000 & 0.2848 & 2.2152 \\ 0 & 0.2382 & 0.8727 & 0.9908 & 1.2290 \end{bmatrix}. \tag{11}$$

Table 6
Parameters of all the dynamic weights

| Input item $x_i$ | Base value $w_i$ | Breadth $B_i$ |
|---|---|---|
| $x_1$ | 1.3015 | 2.2103 |
| $x_2$ | 1.3817 | 2.1729 |
| $x_3$ | 0.6970 | 0.3151 |
| $x_4$ | 0.7018 | 0.2852 |
| $x_5$ | 0.0006 | 0.2028 |
| $x_6$ | 0.0003 | 0.1946 |

The control objective is to transport the payload to the desired position,

$$\begin{bmatrix} x^d & \dot{x}^d & \theta_1^d & \dot{\theta}_1^d & \theta_2^d & \dot{\theta}_2^d \end{bmatrix}^T = \begin{bmatrix} 0.8 & 0 & 0 & 0 & 0 & 0 \end{bmatrix}^T,$$

from the initial position,

$$\begin{bmatrix} x^0 & \dot{x}^0 & \theta_1^0 & \dot{\theta}_1^0 & \theta_2^0 & \dot{\theta}_2^0 \end{bmatrix}^T = \begin{bmatrix} 0 & 0 & 0 & 0 & 0 & 0 \end{bmatrix}^T.$$

Meanwhile, the control system must suppress the natural double-pendulum motions of the hook and payload.

Compared with the SIRMs fuzzy controller and the convolved input-shaping-based (CIS) SIRMs fuzzy controller, Fig. 5 illustrated the control performance of the simultaneous input-shaping-based (SIS) SIRMs fuzzy controller. The curves in Fig. 5a show the trolley position performance via the three controllers. All the three control systems can transport the payload to the desired position, where the SIRMs fuzzy control system has the largest overshooting among the three control systems and the other two control systems on the index almost make on difference.

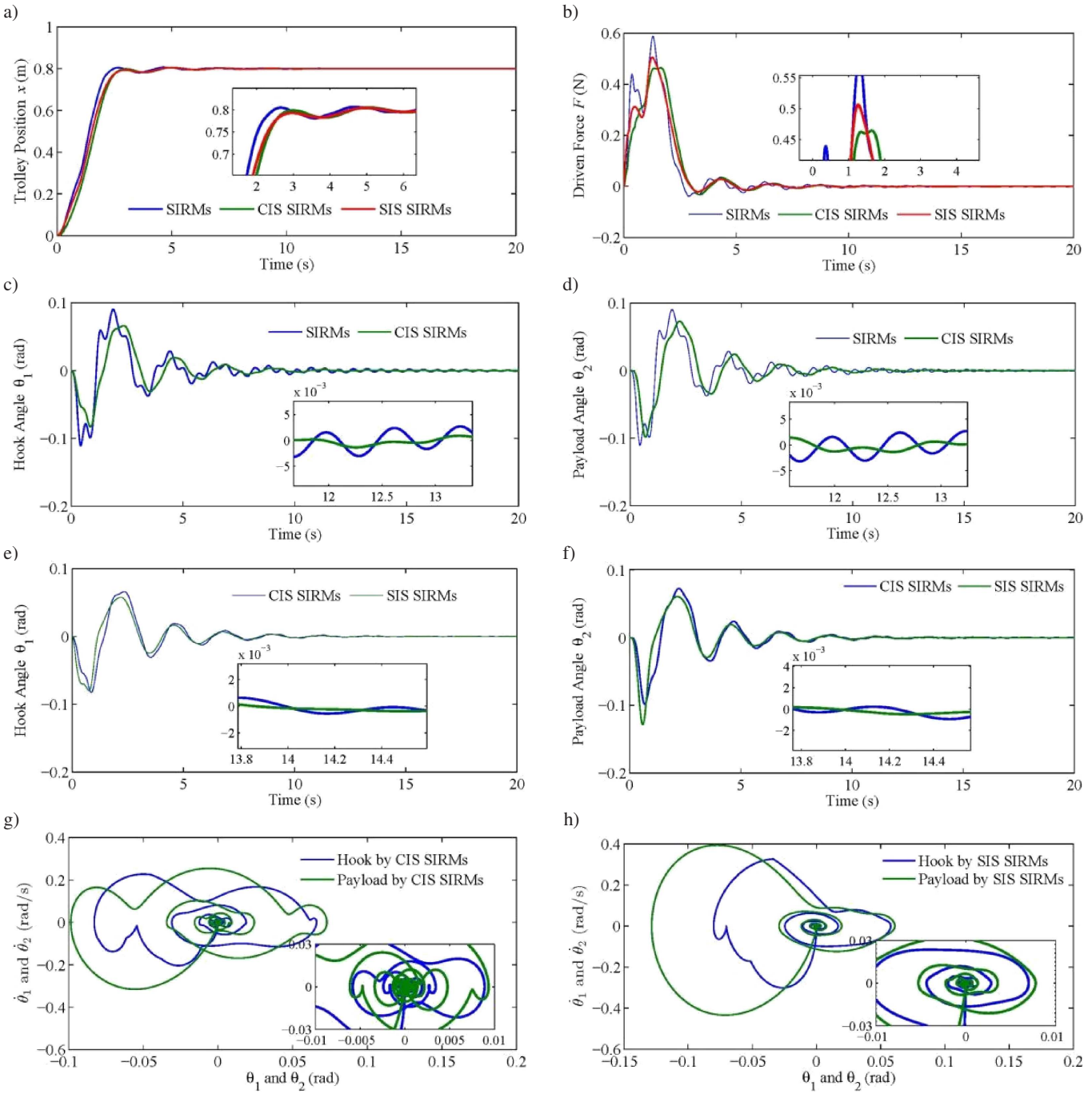


Fig. 5. Comparison of simulation results. a) Trolley position $x$ by the three controllers, b) driven force $F$ by the three controllers, c) Hook angle $\theta_1$ by the SIRMs and CIS SIRMs controllers, d) payload angle $\theta_2$ by the SIRMs and CIS SIRMs controllers, e) Hook angle $\theta_1$ by the CIS SIRMs and SIS SIRMs controllers, f) payload angle $\theta_2$ by the CIS SIRMs and SIS SIRMs controllers, g) phase trajectories of the hook and payload by the CIS SIRMs controller, h) phase trajectories of the hook and payload by the SIS SIRMs controller

The plots in Fig. 5b display the comparison of the driven force via the three controllers. The curve via the SIRMs fuzzy controller sometimes has to swing back and forth to suppress the double-pendulum motions. The control outputs of the CIS and SIS SIRMs fuzzy control systems are smooth, where the SIS SIRMs fuzzy control system has a slightly larger overshooting.

In Fig. 5c–f, the two input-shaping-based SIRMs fuzzy controllers are apparently better to suppress the natural double-pendulum oscillations of the hook and payload than the SIRMs fuzzy controller. Although the difference between the two input-shaping-based SIRMs fuzzy control systems seems slight in Fig. 5c and 5d, the locally zoomed plots in Fig. 5e and 5f show the SIS SIRMs fuzzy control system has smaller residual vibrations.

To demonstrate the comparison of the two input-shaping-based SIRMs fuzzy controllers, the phase trajectories of the hook and payload are displayed in Fig. 5g and 5h, where the locally zoomed plots show the SIS SIMRs fuzzy control system has smaller swags in the desired position.

Through the above-mentioned comparisons, the input-shaping method is effective to suppress the natural double-pendulum oscillations. It can improve the control performance of the SIRMs fuzzy control system. Concerning the types of shapers, the simultaneous input-shaping-based SIRMs fuzzy control system is faster than the convolved input-shaping-based SIRMs fuzzy control system because the simultaneous input shaper is designed to shape the output of the SIRMs controller in the minimum time.

Generally speaking, $m_1$ is usually unchanged but $m_2$ is always changed under different operating conditions. Moreover, $l_1$ is always changed under hoisting operating conditions. To test the robustness of the presented method against the mass and hook-cable length variations, the physical parameter variations $m_2 \in \left[\begin{array}{cc} 0.2 \text{ kg} & 1.25 \text{ kg} \end{array}\right]$ and $l_1 \in \left[\begin{array}{cc} 0.1 \text{ m} & 0.4 \text{ m} \end{array}\right]$ are taken into accounts, respectively. The mass variation indicates the payload-to-hook mass ratio $R \in \left[\begin{array}{cc} 1/2.5 & 2.5 \end{array}\right]$ and the length variation hints the crane hoists 20%∼80% in length of this nominal hook-cable.

Figure 6 displays the simulation results when $m_2$ is its lower and upper bounds and $m_1$, $l_1$, $l_2$ and the controller parameters are kept unchanged from the nominal system. From Fig. 6, the control system can endure a variation of $-60\sim150\%$ in payload mass. The proposed method possesses good performance and good robust stability against wide payload-mass variations.

Figure 7 displays the simulation results when $l_1$ is its lower and upper bounds and $m_1$, $m_2$, $l_2$ and the controller parameters are kept unchanged from the nominal system. From Fig. 7, the control system can endure a variation of $-80\%\sim-20\%$ in the hook-cable length. The proposed method can still possess a good performance after hoisting operating conditions.

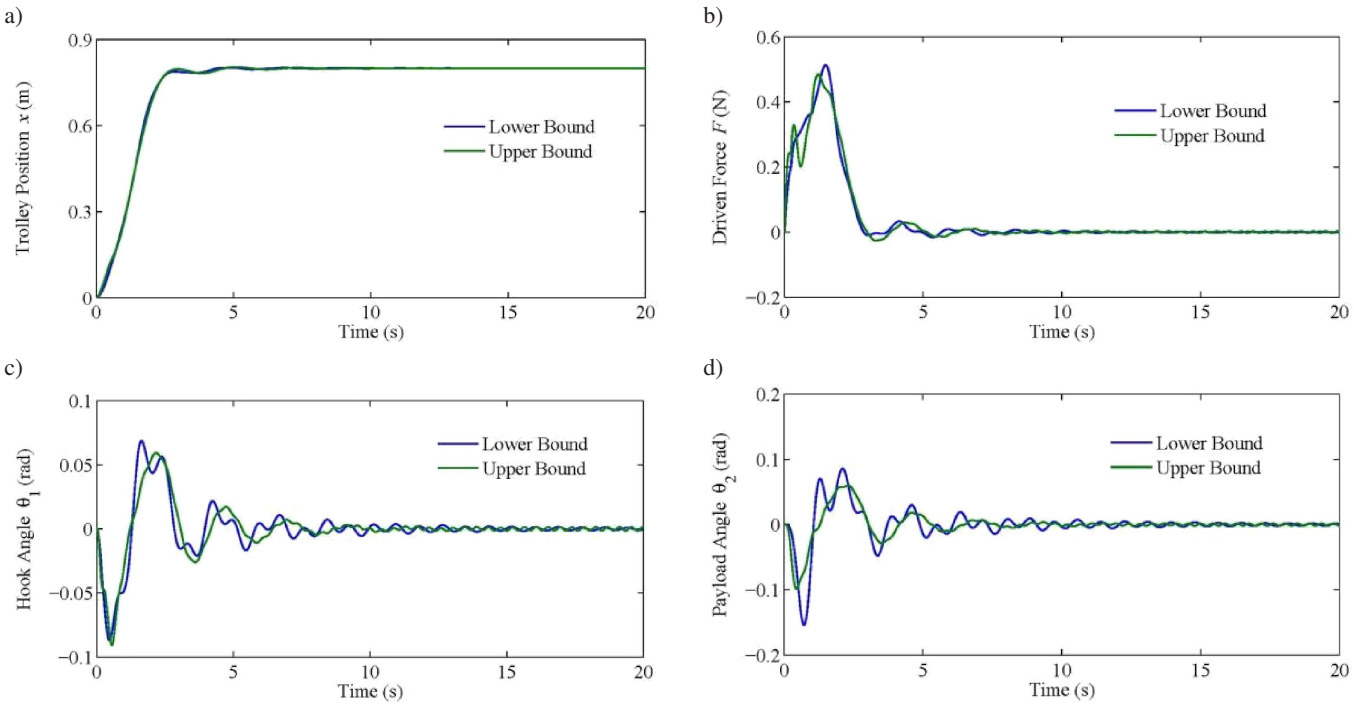


Fig. 6. Results of robustness for the payload mass variation. a) Trolley position $x$, b) driven force $F$, c) Hook angle $\theta_1$, d) payload angle $\theta_2$

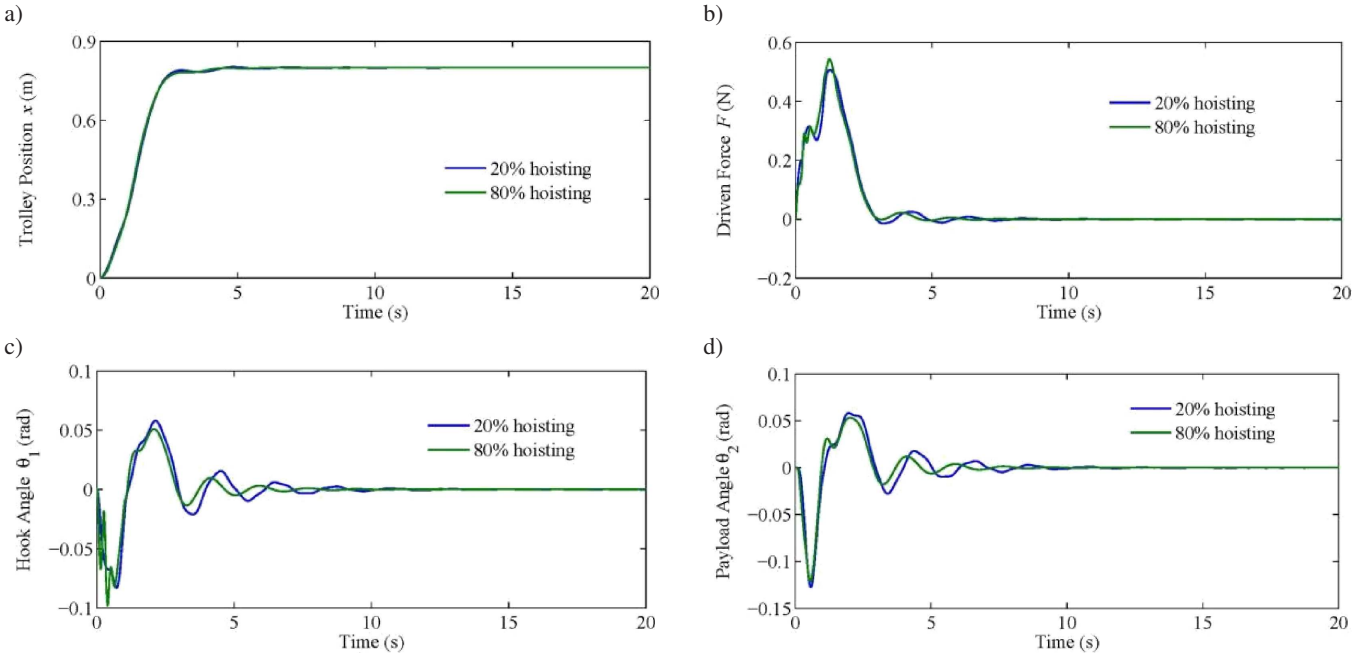


Fig. 7. Results of robustness for the hook-cable length variation. a) Trolley position $x$, b) driven force $F$, c) Hook angle $\theta_1$, d) payload angle $\theta_2$

## 5. Conclusions

This article has designed a simultaneous input-shaping-based SIRMs fuzzy controller for double-pendulum-type overhead cranes. Compared with SIRMs fuzzy control and convolved input-shaping-based SIRMs fuzzy control, the simulation results show the designed controller is superior. The main contributions are to analyze the motions of the double-pendulum overhead cranes and to fuse the input-shaping and SIRMs fuzzy control methods for the transport control problem of double-pendulum-type overhead cranes. The drawback of the presented method is the measurability assumption because the hook and payload angles, especially the payload angle, are difficult to measure. But the presented method is potential with the development of sensor and measuring technologies.

## Appendix

As mentioned, the crane in Fig. 1 contains the high and low frequencies. To suppress the low frequency $f_l$, one Zero Vibration and Derivative (ZVD) shaper $ZVD_{f_l}$ is designed by

$$ZVD_{f_l} = \begin{bmatrix} A_{t_i} \\ t_i \end{bmatrix} = \begin{bmatrix} 1/4 & 1/2 & 1/4 \\ 0 & \rho & 2\rho \end{bmatrix}. \tag{A1}$$

Here $A_{t_i}$ hints an impulse of magnitude $A$ is introduced at time $t_i$ and $\rho = \pi/(\varpi_1)$. To suppress the high frequency $f_h$, the other ZVD shaper $ZVD_{f_h}$ is designed by

$$ZVD_{f_h} = \begin{bmatrix} A_{t_i} \\ t_i \end{bmatrix} = \begin{bmatrix} 1/4 & 1/2 & 1/4 \\ 0 & \sigma & 2\sigma \end{bmatrix}. \tag{A2}$$

Here $\sigma = \pi/(\varpi_2)$. Concerning the crane system, $\sigma$ is usually twice as large as $\rho$. To suppress both the frequencies together, the following convolved shaper $ZVD_{cov}$ can be deduced from (A1) and (A2)

$$ZVD_{cov} = \begin{bmatrix} A_{t_i} \\ t_i \end{bmatrix} = \begin{bmatrix} \frac{1}{16} & \frac{1}{8} & \frac{1}{16} & \frac{1}{8} & \frac{1}{4} & \frac{1}{8} & \frac{1}{16} & \frac{1}{8} & \frac{1}{16} \\ 0 & \rho & 2\rho & \sigma & \rho+\sigma & 2\rho+\sigma & 2\sigma & \rho+2\sigma & 2\rho+2\sigma \end{bmatrix}. \tag{A3}$$

The final control input can be obtained by convolving (A3) and the output of the rate limiter in Fig. 4.

$$F = F_o * ZVD_{cov}. \tag{A4}$$

Here $*$ denotes convolving operator and $F_o$ denotes the output of the rate limiter in Fig. 4.

**Acknowledgements.** This work was supported by the Korea Foundation for Advanced Studies "International Scholar Exchange Fellowship for the academic year of 2013–2014" and the National Natural Science Foundation of China Project under the grant 60904008.

REFERENCES

[1] J. Smoczek, "P1-TS fuzzy scheduling control system design using local pole placement and interval analysis", *Bull. Pol. Ac.: Tech.* 62 (3), 455–464 (2014).

[2] J.Q. Yi, N. Yubazaki, and K. Hirota, "Anti-swing and positioning control of overhead traveling crane", *Information Sciences* 155 (1–2), 1942 (2003).

[3] J. Smoczek, "Interval arithmetic-based fuzzy discrete-time crane control scheme design", *Bull. Pol. Ac.: Tech.* 61 (4), 863–870 (2013).

[4] N. Sun, Y.C. Fang, and X.B. Zhang, "Energy coupling output feedback control of 4-DOF underactuated cranes with saturated inputs", *Automatica* 49 (5), 1318–1325 (2013).

[5] Y.C. Fang, B.J. Ma, P.C. Wang, and X.B. Zhang, "A motion planning-based adaptive control method for an underactuated

crane system", *IEEE Trans. on Control Systems Technology* 20 (1), 241–248 (2012).

[6] X.B. Zhang, Y.C. Fang, and N. Sun, "Minimum-time trajectory planning for underactuated overhead crane systems with state and control constraints", *IEEE Trans. on Industrial Electronics* 61 (12), 6915–6925 (2014).

[7] E. Maleki, W. Singhose, and S.S. Gurleyuk, "Increasing crane payload swing by shaping human operator commands", *IEEE Trans. on Human-Machine Systems* 44 (1), 106–114, (2014).

[8] D.W. Qian, S.W. Tong, and J.Q. Yi, "Adaptive control based on incremental hierarchical sliding mode for overhead crane systems", *Applied Mathematics and Information Sciences* 7 (4), 1359–1364 (2013).

[9] D.W. Qian and J.Q. Yi, "Design of combining sliding mode controller for overhead crane systems", *Int. J. Control and Automation* 6 (1), 131–140 (2013).

[10] M.S. Park, D. Chwa, and M. Eom, "Adaptive sliding-mode antisway control of uncertain overhead cranes with high-speed hoisting motion", *IEEE Trans. on Fuzzy Systems* 22 (5), 1262–1271 (2014).

[11] E.M. Abdel-Rahman, A.H. Nayfeh, and Z.N. Masoud, "Dynamics and control of cranes: a review", *J. Vibration and Control* 9 (7), 863–908 (2003).

[12] W.E. Singhose and S.T. Towell, "Double-pendulum gantry crane dynamics and control", *Proc. IEEE Conf. on Control Applications* 1, 1205–1209 (1998).

[13] W. Singhose, D.R. Kim, and M. Kenison, "Input shaping control of double-pendulum bridge crane oscillations", *J. Dynamic Systems, Measurement and Control* 130 (3), DOI: 10.1115/1.2907363 (2008).

[14] S. Lahres, H. Aschemann, O. Sawodny, and E.P. Hofer, "Crane automation by decoupling control of a double pendulum using two translational actuators", *Proc. American Control Conf.* 1, 1052–1056 (2000).

[15] D.T. Liu, W.P. Guo, and J.Q. Yi, "Dynamics and GA-based stable control for a class of underactuated mechanical systems", *Int. J. Control, Automation and Systems* 6 (1), 35–43 (2008).

[16] W. O'Connor and H. Habibi, "Gantry crane control of a double-pendulum, distributed-mass load, using mechanical wave concepts", *Mechanical Sciences* 4b (2), 251–261 (2013).

[17] L.A. Tuan and S.G. Lee, "Sliding mode controls of double-pendulum crane systems", *J. Mechanical Science and Technology* 27 (6), 1863–1873 (2013).

[18] Y. Dong, Z. Wang, Z. Feng, and J. Cheng, "Incremental sliding mode control for double-pendulum-type overhead crane system", *Proc. 27th Chinese Control Conf.* 1, 368–371 (2008).

[19] J. Vaughan, D.R. Kim, and W. Singhose, "Control of tower cranes with double- pendulum payload dynamics", *IEEE Trans Control Systems Technology* 18 (6), 1345–1358 (2010).

[20] D.R. Kim and W. Singhose, "Performance studies of human operators driving double- pendulum bridge cranes", *Control Engineering Practice* 18 (6), 567–576 (2010).

[21] E. Maleki and W. Singhose, "Swing dynamics and input-shaping control of human-operated double-pendulum boom cranes", *J. Computational and Nonlinear Dynamics* 7 (3) DOI:10.1115/1.4005933 (2012).

[22] D. Blackburn, W. Singhose, and J. Kitchen, "Command shaping for nonlinear crane dynamics", *J. Vibration and Control* 16 (4), 1–25 (2010).

[23] Z. Masoud, K. Alhazza, E. Abu-Nada, and M. Majeed, "A hybrid command-shaper for double-pendulum overhead cranes", *J. Vibration and Control* 20 (1), 24–37 (2014).

[24] M. Adeli, S.H. Zarabadi, H. Zarabadipour, and M.A. Shoorehdeli, "Design of a parallel distributed fuzzy LQR controller for double-pendulum-type overhead cranes", *Proc. IEEE Int. Conf. on Control System, Computing and Engineering* 1, 62–67 (2011).

[25] A. Niewiadomski and M. Kacprowicz, "Higher order fuzzy logic in controlling selective catalytic reduction systems", *Bull. Pol. Ac.: Tech.* 62 (4), 743–750 (2014).

[26] S. Osowski, K. Brudzewski, and L.T. Hoai, "Modified neuro-fuzzy TSK network and its application in electronic nose", *Bull. Pol. Ac.: Tech.* 61 (3), 675–680 (2013).

[27] J. Yi, N. Yubazaki, and K. Hirota, "A proposal of SIRMs dynamically connected fuzzy inference model for plural input fuzzy control", *Fuzzy Sets and Systems* 125 (1), 79–92 (2002).

[28] H. Seki and M. Mizumoto, "SIRMs connected fuzzy inference method adopting emphasis and suppression", *Fuzzy Sets and Systems* 215 (16), 112–126 (2013).

[29] S.W. Tong and D.W. Qian, "Control of a fuel cell based on the SIRMs fuzzy inference model", *Int. J. Hydrogen Energy* 38 (10), 4124–4131 (2013).

[30] S.H. Lau, C.K. Ng, and K.M. Tay, "Data-driven SIRMs-connected FIS for prediction of external tendon stress", *Computers and Concrete, Int. J.* 15 (1), 55–71 (2015).

[31] L. Cheng, Z.G. Hou, M. Tan, and W. Zhang, "Tracking control of a closed-chain five-bar robot with two degrees of freedom by integration of approximation-based approach and mechanical design", *IEEE Trans. Systems, Man, and Cybernetics, Part B: Cybernetics* 42 (5), 1470–1479 (2012).